Spontaneous structural pattern formation at the nanometre scale in kinetically restricted homoepitaxy on vicinal surfaces

2003 J. Phys.: Condens. Matter 15 S3227

(http://iopscience.iop.org/0953-8984/15/47/003)

INSTITUTE OF PHYSICS PUBLISHING JOURNAL OF PHYSICS: CONDENSED MATTER

J. Phys.: Condens. Matter **15** (2003) S3227–S3240 PII: S0953-8984(03)70838-8

Spontaneous structural pattern formation at the nanometre scale in kinetically restricted homoepitaxy on vicinal surfaces

N Néel, T Maroutian, L Douillard and H-J Ernst

CEA Saclay, DSM/Drecam/Spcsi, 91191 Gif Sur Yvette, France

Received 22 October 2003
Published 14 November 2003
Online at stacks.iop.org/JPhysCM/15/S3227

Abstract

The concept of spontaneous pattern formation in epitaxial growth is currently actively explored as a promising pathway for lateral nanostructuring of surfaces. Often, the origin of self-organization is traced back to the presence of an excess energy barrier for adatom diffusion associated with asymmetric features in the crystalline structure, the Ehrlich–Schwöbel barrier. Upon growth of Cu on vicinal Cu surfaces at moderate substrate temperatures a step-meandering instability develops, resulting in an in-plane patterning of the surfaces at the nanometre scale with a temperature- and flux-dependent characteristic wavelength. This meandering instability is superseded by a step-bunching instability during growth at higher temperatures. Specifically, the meandering instability acts as a precursor to the bunching instability, indicating that a one-dimensional treatment of bunching in step flow growth is not sufficient. These nanostructured surfaces might be used as templates in order to guide the growth of materials which do not show spontaneous self-organization.

(Some figures in this article are in colour only in the electronic version)

1. Introduction

Spontaneous pattern formation in kinetically restricted homoepitaxy, erosion of surfaces by ion bombardment or strain-influenced heteroepitaxial growth is currently actively explored as a promising low-cost alternative pathway for planar nanostructuring of surfaces with respect to lithography-based schemes.

This approach demands a detailed understanding, at the atomic scale, of pertinent kinetic mechanisms, such as incorporation, diffusion, nucleation or coalescence of adatoms in the growing thin film. A skillful exploitation of the energetic hierarchy in these processes translates, through spontaneous self-organization of the surfaces, into the appearance of a periodic, lateral arrangement of nanostructures with specific geometry on a scale 5–50 nm. In this way, a high density of identical nano-objects can be produced in a parallel process.

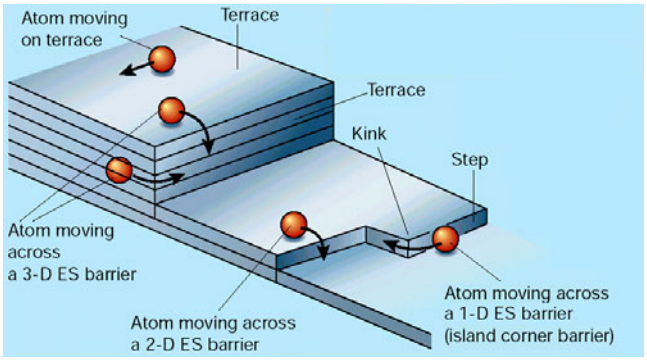

Figure 1. 'The thin-film cliffhanger' (adapted from [2]). The thin-film surface consists of terraces separated by steps; a kink is a step on a step. Atoms travelling over steps (which are also the borders of nucleated islands) must overcome an excess energy barrier for diffusion, the 2D ES barrier. Atoms moving along a step must overcome the 1D ES barrier, across facets the 3D ES barrier.

The deposition of Cu on singular and vicinal Cu surfaces illustrates this approach, using scanning tunnelling microscopy (STM) and helium atom beam scattering (HAS) as structural probes. Our observations underline the importance of the so-called Ehrlich–Schwöbel barrier (ES) (an excess energy barrier for adatom diffusion over steps, kinks or 'cliffs'), a basic physical concept that languished for more than 20 years [1] until the advent of real time, atomic scale structural probes revealed that it is key in governing thin film growth [2].

Its origin can be traced back to asymmetric features in the crystalline structure. The terrace-step-kink model of Burton *et al* [3] describes the atomic-scale morphology of a growing thin-film surface (figure 1). When an atom lands on the surface, it diffuses along the terrace formed by that film layer, trying to find the optimum place to settle, frequently a lower terrace. As it reaches the edge of the terrace, a step, it suddenly has fewer neighbours, and the resulting decrease in the binding energy translates into an excess energy barrier for diffusion over the edge. This hinders the descent of atoms to lower levels, and increases thereby the probability of nucleation and growth of a new layer on top of that terrace. This way, pyramid-like structures, for example in the growth of Cu on Cu(001), are formed with their base oriented along the close-packed ⟨110⟩ directions [4].

The concept of the two-dimensional (2D) ES barrier extends also to other dimensions. As figure 1 shows, a step separates one terrace from another; a kink is a step in a step. Thus, by the same token an atom moving along a step should feel an excess energy barrier associated with the kink preventing it crossing because of its reduced coordination number. This is the one-dimensional (1D) analogue of the ES barrier. Interestingly—and not obvious to envision intuitively—it can also induce the formation of pyramid-like structures in the growth on fcc (001) surfaces [5], this time, however, with their base rotated by 45° with respect to the close-packed directions.

The presence of ES barriers has significant influence on the morphology in the growth on vicinal surfaces as well. These are surfaces which ideally are made up of a regular arrangement of straight steps delimiting terraces whose extension is imposed by a chosen miscut angle with respect to a high symmetry direction; see figure 2. At sufficiently high substrate temperatures and sufficiently low incoming adatom flux, growth does not proceed by nucleation, island formation and coalescence on terraces, but by direct incorporation of adatoms to these pre-existing steps. The thin film grows in the so-called step flow mode. Atoms attach

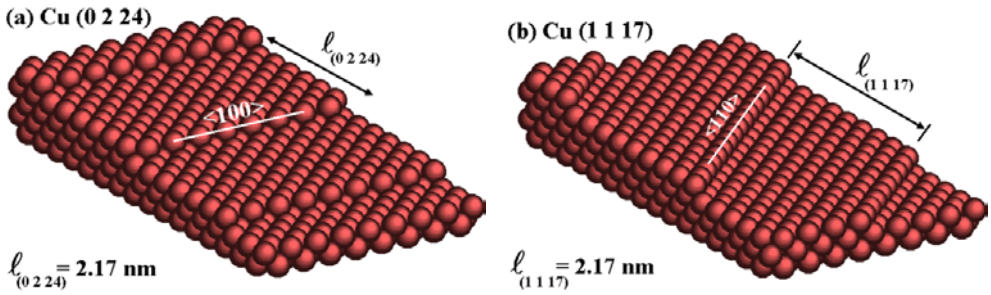

Figure 2. Ball model of fcc vicinal surfaces. The surfaces consist of regularly spaced steps separating low-index terraces. (a) the Cu(0 2 24) surface, consisting of (001) terraces and steps oriented along the open ⟨100⟩ direction, and (b) the Cu(1 1 17) surface, with (001) terraces and steps oriented along the close-packed ⟨110⟩ direction. The surfaces have identical terrace extensions.

to ascending and descending steps, which thereby advance along the step train direction with a velocity proportional to the widths of the adjacent terraces. Originally, this growth mode has been thought to produce perfect layer by layer growth, but unstable step flow has often been encountered: initially straight steps develop a modulated structure (meandering), or the initially equally spaced steps group together (bunching).

It has been shown both theoretically [6, 7] and experimentally [8] that ES barriers are the source of the step *meandering* instability. The presence of the 2D ES barrier in straight steps stabilizes [1] a vicinal surface against step *bunching*. Indeed, in this case, atoms attach preferentially to ascending steps, so that step velocities are mostly determined by the width of their preceding terraces. Consequently, step advancement is controlled by a negative feedback, so that any fluctuation in the terrace widths during growth gets suppressed. Conversely, bunching occurs, when atoms attach preferentially to descending steps due to the presence of an 'inverse' 2D ES (IES) barrier. Thus, meandering and bunching instabilities in the same system are *a priori* mutually exclusive.

2. The meandering instability

In the step flow growth mode, adatoms can be incorporated to ascending or to descending steps. The presence of the 2D ES barrier introduces an asymmetry in the probability for attachment, which, as predicted by Bales and Zangwill [6], results in a transverse in-phase meandering of steps with a characteristic, temperature- and flux-dependent wavelength. Due to the higher probability for a diffusing adatom to stick to already advanced parts of a step, protuberances grow faster in the presence of the 2D ES barrier when steps advance. This destabilizing effect alone would cause perturbations of any wavelength to grow. In a thermodynamic picture, as the amplitude of the fluctuation increases, so does the step length and thus the step free energy. A capillary-induced smoothing follows, either mediated by diffusion of adatoms along step edges, or evaporation of atoms from steps onto terraces, diffusion and recondensation. Therefore, within the framework of a linear stability analysis a critical wavelength naturally emerges from the balance between these effects, leading to a well defined structural modulation of the initially straight step edges. We note that recently, Pierre-Louis *et al* [7] found that quite similar structural patterns are formed through unstable growth initiated by the presence of the 1D ES barrier limiting mass transport along step edges.

Our STM experiments provide first quantitative information on the meandering characteristics and its controlling parameters [8]. Figure 3 shows the morphologies of the

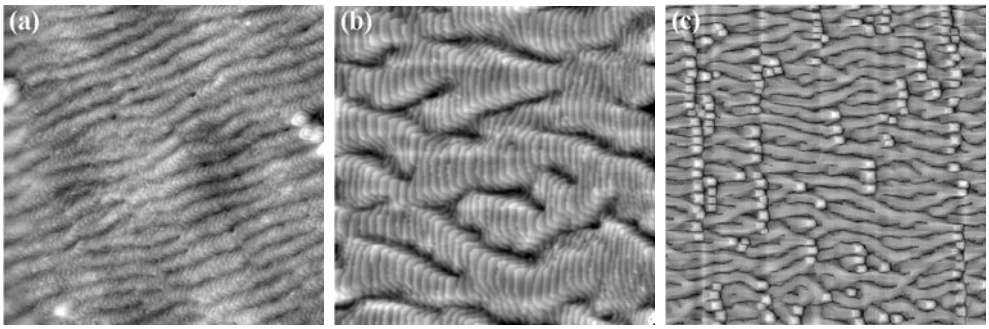

Figure 3. STM topographs of the Cu(0 2 24) (a) and the Cu(1 1 17) (b) surfaces after homoepitaxial step flow in the meandering instability regime. $\Theta = 20$ ML, $F = 3 \times 10^{-3}$ ML s^{-1}, $T = 250$ K, size 135 nm × 135 nm (a), $\Theta = 18$ ML, $F = 5 \times 10^{-3}$ ML s^{-1}, $T = 280$ K, size 85 nm × 85 nm (b). (c) Shows a large-scale image of Cu(1 1 17) after step flow at $\Theta = 80$ ML, $F = 2 \times 10^{-2}$ ML s^{-1}, $T = 285$ K, size 400 nm × 400 nm. Here and for all subsequently shown topographs, the sample has been quenched to $T < 150$ K prior to imaging in order to freeze in the thin-film morphology. Tunnelling parameters are set to around bias $\Delta V \approx -1$ V and current $I \approx 1$ nA.

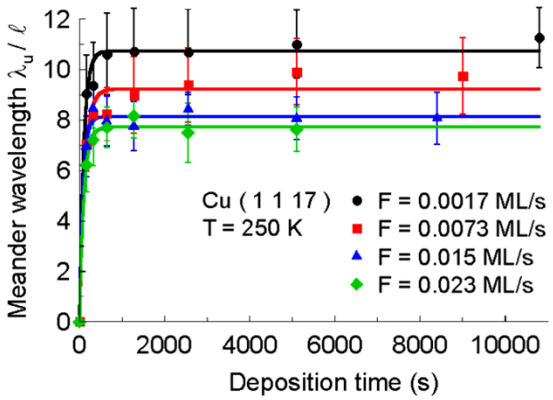

Figure 4. Meandering wavelength λ_u as a function of deposition time for different incident fluxes F on Cu(1 1 17) at $T = 250$ K. λ_u is expressed in units of the mean terrace width ℓ.

Cu(0 2 24) and the Cu(1 1 17) surface after deposition of about 20 ML Cu in the step flow mode. These surfaces have identical terrace widths, but their step orientation differs by 45°; see figure 2. This choice allows us to identify and compare kinetic key parameters associated with the detailed atomic scale step structure.

At around room temperature, in both cases distinctive periodic structural patterns ('ripples', or 'trenches') are formed due to the in-phase adjustment of meandering steps, and a temperature-dependent, characteristic wavelength (the distance between 'ripples') emerges [8] (figures 3(a), (b)). It is worth noting that the characteristic wavelength is stationary during step flow of the meandered morphology, apart from the very early stages during which the individual step modulations adjust to a collective and coherent in-phase meander, see figure 4, and that the initial inter-step distance is preserved. We note that this morphology persists for coverages as high as 250 ML; the predicted transition [9] to a mound-like morphology with increasing coverage has not been observed so far.

The selected wavelength appears to be robust: figures 5(a)–(d) show the resulting morphology after two step flow sequences, at first after deposition at low temperature

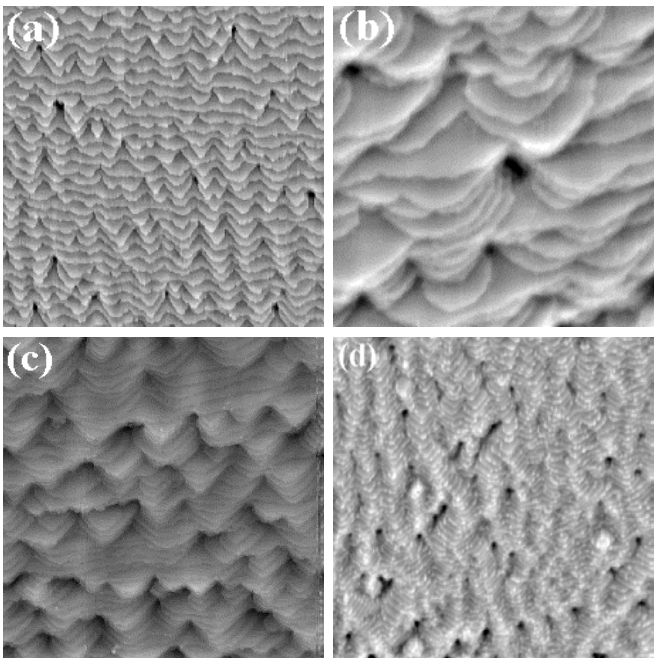

Figure 5. Topographic images of the Cu(0 2 24) surface after two subsequent step flow growth sequences, first after deposition of $\Theta = 10$ ML at $T \approx 255$ K (a), and subsequently onto that meandered morphology another 10 ML at $T \approx 340$ K (b). The incident flux is $F = 3 \times 10^{-3}$ ML s^{-1}; in (c) and (d) the order of sequences is reversed. The selected wavelength locks into the value obtained for growth starting from the pristine surface in both cases. Dimensions are 70 nm × 70 nm (a) and (b), 160 nm × 160 nm (c), and 100 nm × 100 nm (d).

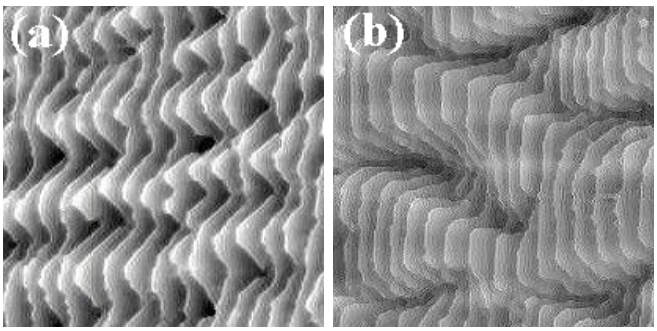

Figure 6. 'Zoom' into the ledge configuration in the meandering instability regime on (a) Cu(0 2 24) and (b) Cu(1 1 17). $\Theta = 9$ ML, $F = 3 \times 10^{-3}$ ML s^{-1}, $T = 245$ K (a), and $\Theta = 18$ ML, $F = 5 \times 10^{-3}$ ML s^{-1}, $T = 280$ K (b). The size of the images is 40 nm × 40 nm.

(figure 5(a)) starting from the pristine surface and subsequently onto the meandered topography at higher temperature (figure 5(b)), or vice versa (figures 5(c), (d)): the system always adapts to those patterns that are observed for deposition on the pristine surface at that given temperature.

A close inspection of the meandered step geometry reveals (figures 6(a), (b)) that the ledge configuration locks into the close-packed ⟨110⟩ directions in both cases, resulting in a 'sawtooth (triangular)' appearance on Cu(0 2 24) and a 'stacked (nearly rectangular)' appearance on Cu(1 1 17). Back-to-front symmetry [10] is observed only for Cu(0 2 24). In contrast, for

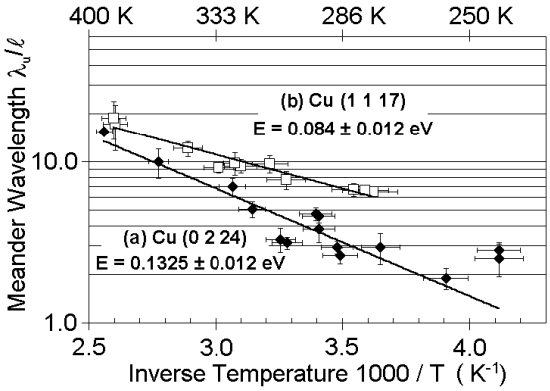

Figure 7. Selected meandering wavelength λ_u as a function of inverse temperature. λ_u is expressed in units of the mean terrace width ℓ. (a) Cu(0 2 24), $\Theta = 5$ ML, $F = 3 \times 10^{-3}$ ML s^{-1} (black diamonds), and (b) Cu(1 1 17), $\Theta = 18$ ML, $F = 3 \times 10^{-3}$ ML s^{-1} (open squares). The indicated energies correspond to the slopes obtained within an Arrhenius-type description excluding the two data points at the lowest temperatures for Cu(0 2 24).

Cu(1 1 17), the ledge profile is asymmetric right from the outset. In any case, the morphology can be reverted to that of the pristine equilibrium structure simply by annealing the surfaces to 700 K.

Is this meandering instability due to the presence of the 2D ES barrier, the 1D ES barrier, or both? On the one hand, Monte Carlo simulations [7, 11, 12] supported by analytical theory [7] demonstrate that if there is competing action of the barriers, the 2D ES will be of no importance for fcc surfaces with steps oriented along the close-packed ⟨110⟩ directions, at least at the length and timescales considered in the simulations. On the other hand, the presence of the 1D ES barrier should stabilize the Cu(0 2 24) surface against meandering [7, 11, 12], contrary to experimental evidence, leaving the 2D ES barrier as source for the meandering instability on this surface.

While qualitatively our experimental observations are in line with this picture, quantitative agreement with current standard theories is lacking. Specifically, the observed temperature-dependent absolute values of the characteristic wavelength, depicted in figure 7, are, for both surfaces, far different from predicted [8], by assuming either the presence of the 2D or the 1D barrier, and taking into account that smoothing proceeds by mass transport along *meandered* step edges [8, 13] in both cases within the temperature range covered by our experiments.

A unified, coherent picture might emerge, if we assume that the meandering wavelength is set by initial nucleation and formation of compact 1D islands on *straight* step edges. At that stage, a 1D nucleation length is defined as [14]

$$L_n = (12a^3 D_s/F\ell)^{1/4} \tag{1}$$

where a denotes the surface lattice constant, F the adatom flux, ℓ the initial inter-step distance, and D_s the diffusion coefficient along a straight ⟨110⟩ or ⟨100⟩ step edge, respectively. The nucleation length equals roughly the size of the 1D islands. If they are larger than the critical wavelength generated through the standard mechanisms by either the presence of the 1D or 2D ES barrier, then these smaller protrusions may not develop at the initial stage of step flow. Experimentally, we observe that the wavelength is invariable during step advancement (figure 4). Therefore, the selected wavelength set by the nucleation length prevails, and the system does not seem to cross over to the 'standard' critical wavelength during step flow growth later on.

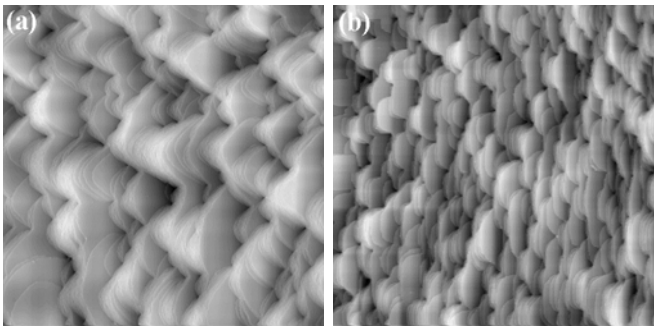

Figure 8. Morphology within the bunching regime on (a) Cu(0 2 24) and (b) Cu(1 1 17). $\Theta = 32$ ML, $F = 2 \times 10^{-2}$ ML s^{-1}, $T = 450$ K, (a), and $\Theta = 20$ ML, $F = 2 \times 10^{-2}$ ML s^{-1}, $T = 450$ K. The size is 330 nm $\times$ 330 nm for both images.

Activation energies for diffusion along straight steps are supposed to be often smaller with respect to energies for diffusion along meandered, kinked steps. Therefore, the requirement that the 1D nucleation length supersedes the 'standard' critical wavelength is commonly fulfilled. Assuming an Arrhenius behaviour for the diffusion coefficient along a straight step, we determine the activation energies and pre-exponential factors with equation (1) from our experimental data to be $E = 0.34 \pm 0.05$ eV and $D_0 = 1.5 \times 10^{-7}$ cm^2 s^{-1} for diffusion along a straight $\langle 110 \rangle$ step, and $E = 0.53 \pm 0.05$ eV and $D_0 = 2 \times 10^{-5}$ cm^2 s^{-1} for the $\langle 100 \rangle$ step edge. These values compare favourably with independently obtained ones [13].

If one accepts that this agreement is not fortuitous, we may speculate on the following picture: the meandering instabilities generate a concerted modulation of advancing steps, the wavelength of which is at variance with the 'standard' scenario, but invariably imposed by the 1D nucleation length on initially straight step edges. The shape of the 'ripples' evolves towards a ledge configuration with close-packed $\langle 110 \rangle$ step orientations, and preserves these low energy orientations during step advancement. Theories [7, 10, 11] reveal that the meandering wavelength in fact equals the 1D nucleation length, when the meandering instability is induced by the presence of a strong (comparable to the kink creation energy) 1D ES barrier, and smoothing proceeds by the stochastic nature of nucleation, and not by mass transport along step edges. So far, there is no direct evidence available for a strong 1D ES barrier in the class of vicinal surfaces Cu($11n$), $n = 5, 9, 17$. Moreover, as mentioned above, by symmetry, the 1D ES barrier cannot initiate unstable step flow on Cu(0 2 24), leaving the 2D ES barrier as the source for the meandering instability on this surface with its open step orientation. Presumably it initiates unstable step flow in Cu($11n$) as well, because, at comparable incident fluxes and surface temperatures, the observed growth instability on the singular Cu(0 0 1) surface [4] leads to the formation of pyramid-like structures whose bases are oriented along the close-packed $\langle 110 \rangle$ directions, and not, as predicted [5], along the $\langle 100 \rangle$ directions if the 1D ES barrier were operative.

3. The bunching instability

As reported above, on both surfaces a meandering instability develops during step flow at around and below room temperature deposition. In contrast, and unexpectedly, we find [15] that step flow at higher temperatures does not result in concerted step meandering, but in the formation of large (001) terraces separated by curved, bunched regions of reduced inter-step distance; see the STM topographs in figure 8. Step advancement during growth develops a

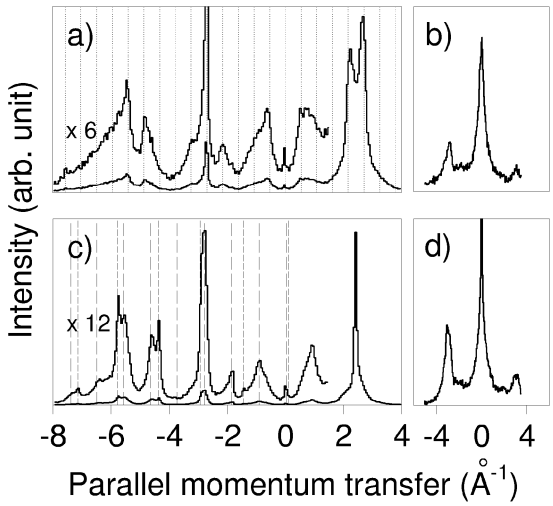

Figure 9. HAS angular distributions of the Cu(119) surface after step flow growth in the meandering (upper panel), and in the bunching (lower panel) regimes for diffraction perpendicular (a), (c), and parallel (b), (d) to the average step direction $[1\bar{1}0]$. (a), (c) are sensitive to the inter-step spacing, (b), (d) to meandering. In both cases the flux was set to $F = 10^{-2}$ ML s^{-1}, with 15 ML deposited at $T = 190$ K (a), (b) and 20 ML deposited at $T = 400$ K (c), (d). The incident wavevector is $k_i = 11.2$ Å^{-1}, the angle between source and detector is set to $\Theta_{SD} = 92°$ (a), (c) and $\Theta_{SD} = 104°$ (b), (d). In (a) not all diffraction peaks related to the (119) step grating (dotted lines) are visible because of strongly meandering steps and the chosen scattering conditions in order to highlight the 'rainbow doublet' at around $K \approx 2.5$ Å^{-1}. In (c) the peaks are no longer related to the (119) grating, but correspond to patches of Cu(113) (short dashed lines), Cu(115) (long dashed lines), and (001) orientation (not labelled). The spectra have been recorded after a quench to $T < 140$ K in order to avoid structural change of the morphology.

bunching instability (faceting), which results in a 'scaly' morphology. A lateral modulation of bunched steps is still visible, reminiscent of the meandering instability observed at low deposition temperatures; however, extended phase correlation is lost. We note that, as in the meandering regime, annealing the surfaces to about 700 K restores the pristine morphology. Therefore, the observed instabilities are purely kinetic in origin and out of equilibrium phenomena.

This unexpected growth scenario, the coexistence of the meandering and the bunching instabilities, has been found in a whole class of Cu vicinal surfaces, Cu$(11n)$, $n = 5, 9, 17$, as well as on Cu(0 2 24). In the following we present detailed, representative results of Cu(119), using HAS and STM as complementary reciprocal and real space atomic scale structural probes.

HAS angular distributions recorded along the step train direction $[\bar{1}\bar{1}0]$ are sensitive to the inter-step spacing. Angular distributions recorded in the meandering regime (growth at low substrate temperatures), figure 9(a), show diffraction peaks exclusively related to the (119) grating, which assert that the inter-step distance of the pristine surface is preserved during step flow. Meandering is reflected in the broadening of some of the diffraction peaks (figure 9(a)), and in the presence of satellite diffraction peaks recorded along the average step direction $[1\bar{1}0]$, otherwise absent [15] for straight steps (figure 9(b)).

The loss of the inter-step distance of the pristine surface in the bunching regime (growth at high substrate temperatures) is immediately witnessed by the HAS angular distribution recorded along the step train direction $[\bar{1}\bar{1}0]$, which shows diffraction peaks not related to the (119) step grating, figure 9(c). A detailed analysis reveals that the regular step train is

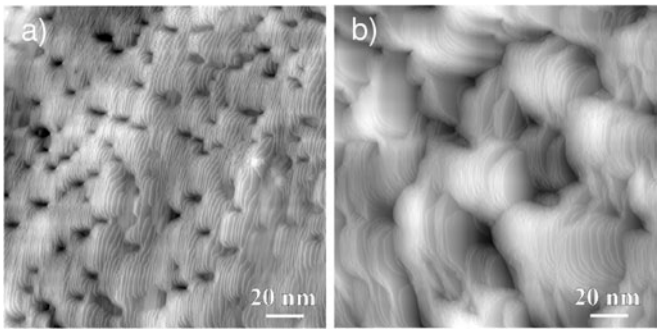

Figure 10. 170 nm × 170 nm STM topographs of the Cu(119) surface after step flow growth in the meandering (a), and in the bunching (b) regimes corresponding to HAS spectra (9a), (b) and (9c), (d), respectively. (a) 15 ML deposited at $T = 230$ K, $F = 10^{-2}$ ML s^{-1}, and (b) 30 ML deposited at $T = 400$ K, $F = 10^{-2}$ ML s^{-1}. Tunnelling parameters are 1 nA current and −0.4 V sample bias.

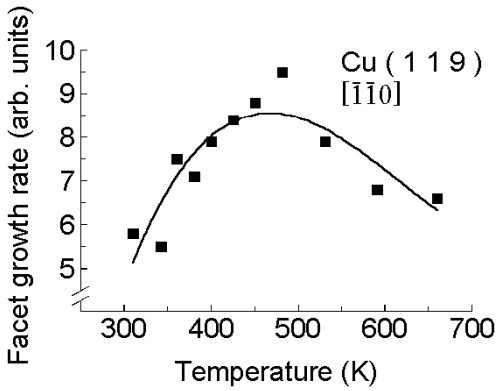

Figure 11. Growth rate of the (001) facets on Cu(119) as a function of substrate temperature, from the (001) diffraction peak (corrected for the Debye–Waller effect) recorded parallel to the step train direction [$\bar{1}\bar{1}0$] during growth. The solid curve is a guide to the eye.

decomposed upon growth into bunches of reduced inter-step distance corresponding locally to Cu(115) and (113) grids, separated by large (001) terraces. The continuing presence of the satellite peaks along the average step direction [$1\bar{1}0$], figure 9(d), asserts that the morphology has a 'scaly' aspect. The corresponding STM topographs are depicted in figures 10(a), (b).

HAS allows us as well to follow the development of the (001) facets with coverage (time) at various deposition temperatures. For this purpose the diffraction peak associated with scattering from the (001) facets has been recorded during step flow growth. The relative proportion of (001) facets on the surface at first rapidly increases with coverage and then, after deposition of 10–20 ML, a slow coarsening regime is reached with stationary size distribution (stationary peak shape) but increasing mean facet size (decreasing peak width). A full account of the time evolution will be given elsewhere [16]. Figure 11 shows the growth rate of the (001) facets in the coarsening regime, which from ≈300 K increases sharply with temperature, while it reduces at the highest deposition temperatures. A bell shape-like curve is thus obtained, which cannot be cast into an Arrhenius-type behaviour.

As outlined in the introduction, meandering and bunching instabilities are *a priori* mutually exclusive, contrary to our experimental finding. A detailed investigation of the transition

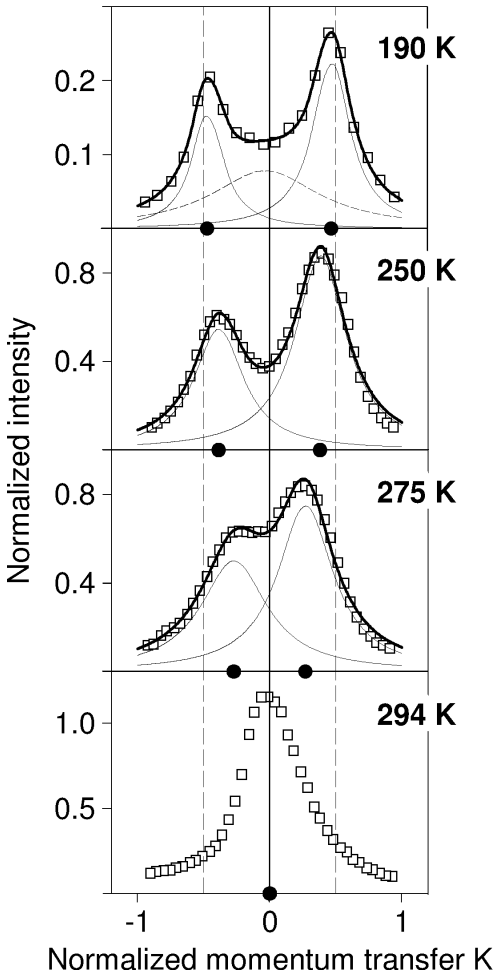

Figure 12. HAS 'rainbow doublet' (see footnote 1) recorded after deposition of 35 ML at $F = 10^{-2}$ ML s^{-1} for temperatures in the range [190 K, 294 K]. (□) experimental data, (thin and thick curves) fitted Lorentzian peaks whose positions are reported as black dots. The shift of the rainbow peaks from their ideal positions at $K = \pm 1/2$ (vertical dashed lines) towards the centre of the (001) Brillouin zone (vertical full line) reflects a smooth transition from a stable step train in the meandering regime with narrow terrace width distribution (190 K) to an unstable in the bunching regime with asymmetric distribution and adjoining (001) facets (294 K). Note that, at $T = 190$ K, an additional peak (short dashed line) has to be introduced to account for the strong meandering of the steps off the $[1\bar{1}0]$ direction.

between the observed meandering and bunching instabilities with temperature might hold the key to understand the origin of their coexistence within the same system.

One imagines that bunching during step advancement starts through the formation of an increasing number of narrow terraces compensating for a few larger ones. The resulting asymmetry in the terrace width distribution can be traced by HAS through a close inspection of diffraction peaks sensitive to destructive interferences between neighbouring terraces ('out-of-phase condition' with respect to (001) terraces)[1] [17]. Figure 12 shows the evolution of the

[1] These peaks are seen in figure 9(a) at around 2.5 Å^{-1} momentum transfer, and as the corresponding scattering angles are close to the miscut angle of the surface, they have greatly enhanced intensities (this is the so-called 'rainbow scattering effect').

'rainbow doublet' (see footnote 1) of Cu(119) with growth temperature. The peak positions inside the doublet shift towards each other and merge finally into the diffraction peak associated with (001) terraces. This continuous shift reflects the expected emerging asymmetry in the terrace width distribution [17], and allows us to locate the 'onset temperature' of the bunching instability between 250 and 275 K. For the present purpose it is important to note that both HAS and STM data indicate the continuous presence of *meandering* steps over this whole temperature range. This is an unambiguous indication of the 2D character of the transition between meandering and bunching. The presence of 2D step profiles is the key element for the bunching instability to develop, indicating that a 1D description as to the origin of step bunching observed at high growth temperatures is insufficient.

The meandering instability can be traced back to the competing presence of the 1D ES and 2D ES barriers [6, 7]. Purely 1D theories, assuming straight step edges [1, 10] exclude the appearance of the bunching instability in the same system, unless, at high temperatures, an IES barrier appears, i.e. the attachment of adatoms to ascending steps becomes kinetically unfavourable or inhibited. This mechanism has originally been invoked for bunching observed in molecular beam epitaxy of GaAs [18]. So far, for non-reconstructed metallic systems, there is no indication that such a process exists. Possibly the 'compensation effect'[2] could produce such a crossover with temperature even in simple metallic systems. In this case, within an Arrhenius-type description, diffusion across steps is characterized not only by an excess energy barrier but also by a larger pre-exponential factor as compared to diffusion on terraces. Thus, a higher attempt frequency could compensate for the excess energy barrier, leading to preferential attachment to descending steps at high temperatures. However, measurements of the surface phonon spectra that are related to the pre-exponential factor exhibit no extra signature[3]. Moreover, and more important, the IES barrier has been shown to stabilize against step meandering [24]. Therefore, the bunched morphology should exhibit *straight* step edges, contrary to the 'scaly' aspect experimentally observed. The '2 particle' model of Pimpinelli *et al* [25] considers growth processes involving two kinds of diffusing entities, a precursor and a growth unit. In the presence of ES barriers, the concerted action of both species may lead to step bunching. This model accounts successfully for the presence of both bunching and meandering in homoepitaxial growth of GaAs [18]. However, it is unclear what species would take the role of the '2nd particle' in the homoepitaxial growth of Cu.

Our reported experimental investigation of the transition during step flow between meandering and faceting points to the fact that a 1D description of the growth might be insufficient. This result joins a recent theory of Politi and Krug [26], who have shown within a full 2D theoretical treatment that diffusion along *meandered* steps may induce a faceting of the surface. They show that a net step edge adatom diffusion current (possibly augmented by the presence of the 1D ES barrier) along *meandered* steps may produce a faceting of the surface. Thus, in this picture, the faceting is a natural consequence of the preceding meandering instability, acting as a precursor. This model accounts also for the observed temperature dependence of the (001) facet growth rate (figure 11) and the fact that the onset temperature for faceting scales with the initial terrace width, as it has been checked explicitly

[2] The 'compensation effect' (the system is not only characterized by a 2D ES barrier, but also by a higher pre-exponential factor for diffusion across steps) [19], could in principle provide the required preferential attachment of adatoms to descending steps at high temperatures. If it would be operative, it can be shown [20] that its influence is restricted to growth on vicinals with very short terrace widths. Also, according to Krug [21], steering [22] might be acting as source as well. It is, however, questionable if this effect is still strong enough at normal incidence deposition (although the inclination of the terrace with respect to the macroscopic surface may enhance its influence). Moreover, it would most likely be canceled out (neutralized or balanced) by the presence of the 2D ES barrier.

[3] One might envision that such a process could be mediated by an anomalous surface phonon spectrum on vicinal Cu surfaces. However, in particular the step localized phonons show the expected behaviour; see [23].

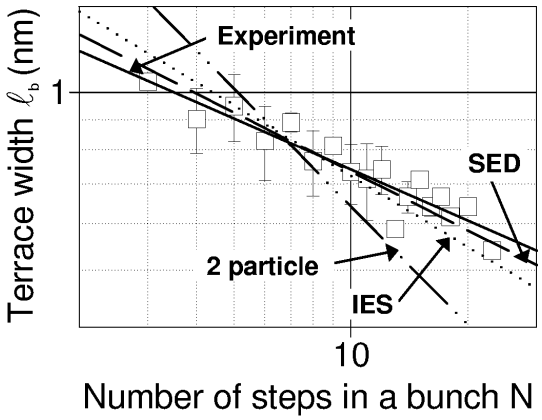

Figure 13. The terrace width ℓ_b within a bunch versus the number of steps N in a bunch for the Cu(119) surface (□). Lines correspond to the power law behaviours $\ell_b \propto N^{-\gamma}$ predicted for different bunching mechanisms [27]: '2 particle model' $\gamma = 2/3$, 'inverse' Schwöbel barrier $\gamma = 2/5$ (IES), and step edge diffusion $\gamma = 1/3$ (SED). For the whole Cu(119) data set, the best fit power law exponent is $\gamma = 0.29 \pm 0.05$; see the text.

with both HAS [15] and STM for the homoepitaxial step flow on Cu($11n$), $n = 5, 9, 17$. The net step current is an activated process (expected to be operative only at relatively high temperatures due to the large activation energies for diffusion along kinked steps) that is linked [10, 14] to the 1D diffusion length L_n, which itself is related to the inter-step distance ℓ via equation (1). Moreover, the stabilizing effect of a 2D ES barrier is favoured by wide terraces [1, 10]. The decrease of the (001) facet growth rate at the highest temperatures (figure 11) could be induced by the creation of additional, thermally activated kinks that slow down diffusion along meandered step edges, or simply by an overall smoothing of the surface due to the activation of kinetic channels that are closed at lower temperatures.

Additional support for this picture comes from our measurements of the mean terrace width ℓ_b within a step bunch, figure 13. According to Pimpinelli *et al* [27], this observable reflects the origin of bunching, through the coupling of step motion via the kinetic-channel-dependent diffusion field between steps. Our experimental data is best described by a power law, whose exponent $\gamma = 0.29$ compares favourably with the theoretical prediction $\gamma = 1/3$ [27] for bunching induced by step edge currents. The analysis of other faceting processes, i.e. the IES effect and the '2 particle' model, reveals power law exponents $\gamma = 2/5$ and $2/3$, respectively [27]. While the latter lies outside the experimental error margin (figure 13), the exponent of the IES mechanism could describe our data as well. But again, this specific mechanism would lead to the appearance of *straight* bunched steps, which are not experimentally observed here. Therefore, the 'inverse' 2D ES barrier (IES) as the source of bunching can be excluded.

4. Summary and outlook

The use of instabilities in kinetically restricted growth is demonstrated to be a promising pathway for lateral nanostructuring of surfaces, including the cases reported here of pre-structured vicinal surfaces. The length scale of the structural patterns is set by the competition between the destabilizing external flux in conjunction with a kinetically limiting component of adatom diffusion, and a stabilizing, smoothing component. As a result, the morphology can be tuned and controlled through the choice of flux, temperature, and substrate, whether singular or vicinal.

This approach to lateral nanostructuring has here been illustrated for the growth of Cu on vicinal Cu surfaces. It is shown that meandering and bunching instabilities can coexist in these systems; in fact, the meandering instability acts as a precursor to the bunching instability. In the temperature and flux range covered by our experiments, homoepitaxial step flow is thus never stable on these surfaces.

As a next step, one might envision to use these nanostructured surfaces as templates in order to guide the growth of other materials which do not show spontaneous self-organization.

Specifically, the recent demonstration of electronic devices based on molecular single crystals as an active component has received much attention [28]. But practical applications for devices require the growth of organic films in a coherent, laterally ordered manner on a variety of substrates. In general, however, organic materials grow in a rather disordered manner on unstructured, flat substrates, thereby degrading seriously their inherently superior electronic properties. The use of properly pre-structured surfaces as templates in order to guide growth might represent a promising pathway for lateral molecular ordering.

Acknowledgments

The technical assistance of P Lavie and F Merlet is highly appreciated. It is a pleasure to acknowledge intense and fruitful discussions with J Krug (Essen), A Pimpinelli (Clermont-Ferrand) and O Pierre-Louis (Grenoble). The calculation of pertinent kinetic parameters for Cu surfaces by M-C Desjonquères, D Spanjaard and C Barreteau (Saclay) has been very helpful.

References

[1] Ehrlich G and Hudda F G 1966 *J. Chem. Phys.* **44** 1039
Schwöbel R L and Shipsey E J 1966 *J. Appl. Phys.* **37** 3682
Schwöbel R L 1969 *J. Appl. Phys.* **40** 614
[2] Lagally M and Zhang Z 2002 *Nature* **417** 907
[3] Burton W K, Cabrera N and Frank F C 1951 *Phil. Trans. R. Soc.* A **243** 299
[4] Ernst H-J *et al* 1994 *Phys. Rev. Lett.* **72** 112
Zuo J-K and Wendelken J 1997 *Phys. Rev. Lett.* **78** 2791
Broeckman P *et al* 2002 *Phys. Rev. Lett.* **89** 146102
[5] Ramana Murty M V and Cooper B H 1999 *Phys. Rev. Lett.* **83** 352
[6] Bales G S and Zangwill A 1990 *Phys. Rev.* B **41** 5500
[7] Pierre-Louis O, D'Orsogna M R and Einstein T L 1999 *Phys. Rev. Lett.* **82** 3661
[8] Maroutian T, Douillard L and Ernst H-J 1999 *Phys. Rev. Lett.* **83** 4353
Maroutian T, Douillard L and Ernst H-J 2001 *Phys. Rev.* B **64** 165401
[9] Rost M, Smilauer P and Krug J 1996 *Surf. Sci.* **369** 393
[10] Politi P *et al* 2000 *Phys. Rep.* **324** 271
Gillet F, Pierre-Louis O and Misbah C 2000 *Eur. Phys. J.* B **18** 519
[11] Rusanen M, Koponen I T, Heinonen J and Ala-Nissila T 2001 *Phys. Rev. Lett.* **86** 5317
[12] Kallunki J, Krug J and Kotrla M 2002 *Phys. Rev.* B **65** 205411
[13] Giesen-Seibert M *et al* 1993 *Phys. Rev. Lett.* **71** 3521
Giesen-Seibert M *et al* 1995 *Surf. Sci.* **329** 47
[14] Politi P and Villain J 1996 *Phys. Rev.* B **54** 5114
[15] Néel N, Maroutian T, Douillard L and Ernst H-J 2003 *Phys. Rev. Lett.* **91** at press
Schwenger L, Folkerts R and Ernst H-J 1997 *Phys. Rev.* B **55** R7406
[16] Maroutian T *et al* 2003 in preparation
[17] Wollschläger J 1997 *Surf. Sci.* **383** 103
Wollschläger J 1997 private communication
[18] Tejedor P *et al* 1999 *Phys. Rev.* B **59** 2341
[19] Boisvert G, Lewis L J and Yelon A 1995 *Phys. Rev. Lett.* **75** 469
[20] Ferrando R 2003 private communication

[21] Krug J 2003 private communication
[22] van Dijken S, Jorritsma L and Poelsema B 1999 *Phys. Rev. Lett.* **82** 4038
[23] Kara A, Staikov P, Rahman T, Radnik J, Biagi R and Ernst H-J 2000 *Phys. Rev.* B **61** 5714
Radnik J and Ernst H-J 1999 *J. Chem. Phys.* **110** 10522
[24] Sato M and Uwaha M 2001 *Surf. Sci.* **493** 494
[25] Pimpinelli A and Videcoq A 2000 *Surf. Sci.* **445** L23
Videcoq A, Vladimirova M and Pimpinelli A 2001 *Appl. Surf. Sci.* **175/176** 140
[26] Politi P and Krug J 2000 *Surf. Sci.* **446** 89
[27] Pimpinelli A, Tonchev V, Videcoq A and Vladimirova M 2002 *Phys. Rev. Lett.* **88** 206103
[28] Meyer zu Heringsdorf F-J, Reuter M C and Tromp R 2001 *Nature* **412** 517